VPAC1 Receptors for Imaging Breast Cancer: A Feasibility Study

Mathew L. Thakur[1,2], Kaijun Zhang[1], Adam Berger[3], Barbara Cavanaugh[1], Sung Kim[1], Chaitra Channappa[1], Andrea J. Frangos[1], Eric Wickstrom[2,4], and Charles M. Intenzo[1]

[1]Department of Radiology, Thomas Jefferson University, Philadelphia, Pennsylvania; [2]Kimmel Cancer Center, Thomas Jefferson University, Philadelphia, Pennsylvania; [3]Department of Surgery, Thomas Jefferson University, Philadelphia, Pennsylvania; and [4]Department of Biochemistry and Molecular Biology, Thomas Jefferson University, Philadelphia, Pennsylvania

VPAC1 encodes G-protein–coupled receptors expressed on all breast cancer (BC) cells at the onset of the disease, but not on benign lesions. Our extensive preclinical studies have shown that ^{64}Cu-TP3805 has a high affinity for VPAC1, is stable in vivo, and has the ability to distinguish spontaneously grown malignant BC masses from benign lesions. Our long-term goal is to develop ^{64}Cu-TP3805 as an agent to perform in vivo histology, to distinguish malignant lesions from benign masses noninvasively and thereby avoid patient morbidity and the excess economic costs of benign biopsies. **Methods:** ^{18}F-FDG obtained commercially served as a control. ^{64}Cu-TP3805 was prepared using a sterile kit containing 20 μg of TP3805. Radiochemical purity and sterility were examined. Nineteen consenting women with histologically proven BC were given 370 MBq of ^{18}F-FDG. One hour later, 6 of these patients were imaged with PET/CT and 13 with positron emission mammography (PEM). Two to 7 d later, 6 PET/CT patients received 111 MBq ($\pm$10%) ($n = 2$), 127 MBq ($\pm$10%) ($n = 2$), or 148 MBq ($\pm$10%) ($n = 2$) of ^{64}Cu-TP3805 and were imaged 2 and 4 h later. Thirteen PEM patients received 148 MBq ($\pm$10%) of ^{64}Cu-TP3805 and were imaged 15 min, 1 h, 2 h, and 4 h later. Standardized uptake value (SUV) was calculated for PET/CT patients, and PUV/BGV (PEM uptake value/background value) was calculated for PEM patients. Tumor volume was also calculated. **Results:** The radiochemical purity of ^{64}Cu-TP3805 was 97% $\pm$ 2%, and specific activity was 44.4 GBq (1.2 Ci)/μmol. In 19 patients, a total of 24 lesions were detected (15 invasive ductal carcinoma, 1 high-grade mammary carcinoma, 3 lobular carcinoma, 1 invasive papilloma, and 4 sentinel lymph nodes). All lesions were unequivocally detected by ^{64}Cu-TP3805 and by ^{18}F-FDG. The average tumor volume as determined by PET/CT with ^{64}Cu-TP3805 was 90.6% $\pm$ 16.1% of that with ^{18}F-FDG PET/CT, and the average SUV was 92% $\pm$ 26.4% of that with ^{18}F-FDG. For PEM, the tumor volume with ^{64}Cu-TP3805 was 113% $\pm$ 37% of that with ^{18}F-FDG and the PUV/BGV ratio was 97.7% $\pm$ 24.5% of that with ^{18}F-FDG. **Conclusion:** ^{64}Cu-TP3805 is worthy of further investigation in patients requiring biopsy of suggestive imaging findings, to further evaluate its ability to distinguish malignant lesions from benign masses noninvasively.

Of the approximately 1.6 million breast biopsies that were performed in the United States in 2011, about 288,130 breast cancers (BCs) were diagnosed (230,480 invasive and 57,650 in situ) (*1,2*), but over 1.3 million of these biopsies resulted in a benign diagnosis. These unnecessary biopsies create significant patient morbidity and potentially unnecessary health care costs. To detect BC, digital mammography, MRI, CT, sonography, ^{18}F-FDG, and ^{99m}Tc-sestamibi have made significant advances. However, all of these modalities have limited specificity, and all continue to produce many false-positive and false-negative results (*3–12*). At an average cost of $5,000–$6,000 for each biopsy, unnecessary benign biopsies represent a serious health care burden. There is a compelling need for an innovative approach that would decrease the number of unnecessary benign biopsies while still detecting the malignancies.

Recent approaches to drug discovery focus on understanding the genesis of diseases and the biomedical pathways that control them at a molecular level. Previous studies have demonstrated that VPAC1 receptors (combined for vasoactive intestinal and pituitary adenylate cyclase activating peptide [PACAP]) are overexpressed in high density on BC (*13*). VPAC1 receptors encode a G protein involved in cell proliferation, cell differentiation, and survival of BC cells. On stroma, normal cells, and benign masses, only a few VPAC1 receptors are expressed (*13–18*).

We therefore hypothesized that a radiolabeled biomolecule with a high affinity for VPAC1 receptors would not only image BC early but also distinguish malignant lesions from benign masses. To validate this hypothesis on a molecular level, a large body of preclinical data was generated (*19–27*). On the basis of their high affinity for VPAC1 receptors, we chose 4 peptide constructs, modified them for radiolabeling with ^{99m}Tc (half-life [$t_{1/2}$], 6 h; γ-energy, 140 keV), and evaluated them for receptor affinity (dissociation constant), receptor specificity, in vivo stability, and tissue distribution (*20–27*). Impetus generated from these results prompted us to label the 4 molecules with β+ (19%, 656 keV) emitting ^{64}Cu ($t_{1/2}$, 12.8 h) for PET. We used N_2S_2 chelating agent, determined dissociation constants, performed tissue distribution studies

in athymic nude mice bearing T47D human BC, performed receptor blocking studies, determined receptor affinity, and examined their stability in vivo (23–27).

After a critical evaluation of these data, we chose a PACAP analog, ^{64}Cu-TP3805, for further evaluation. ^{64}Cu-TP3805 not only imaged all xenografted human BC in athymic nude mice (tumor uptake, 6.35% ± 1.28% injected dose/g at 24 h after injection) but also localized all (n = 8) spontaneously grown BC (5 visible, 1 invisible, and 2 metastatic) lesions in transgenic MMTVneu mice (n = 9) (26). Furthermore, the ^{64}Cu-TP3805 PET images were normal for 2 lesions that had negligible expression of VPAC1 receptors. These were benign histologically as examined by an independent senior pathologist. These 2 benign lesions displayed prominent ^{18}F-FDG images. Among the 8 malignant lesions, only 4 were imaged by ^{18}F-FDG. All malignant lesions (n = 8) were confirmed by histology and expressed VPAC1 receptors as determined by RT-PCR (26). The 2 histologically determined benign lesions had negligible expression of VPAC1 receptors. Spontaneous growth of BC in MMTVneu mice resembled the pathophysiology of human BC. Further evidence of the receptor specificity of ^{64}Cu-TP3805 was obtained by digital autoradiography of human BC specimens, in which ^{64}Cu-TP3805 had nearly 6 times greater uptake of radioactivity (n = 5) than that of benign stroma (24). These highly encouraging data, particularly the ability of the probe to image only malignant lesions with high specificity, prompted us to undertake this study in humans.

In this article, we will describe the feasibility of imaging BC in humans with ^{64}Cu-TP3805 using PET and positron emission mammography (PEM) scanners.

MATERIALS AND METHODS

TP3805 Synthesis and Kit Preparation

Briefly, the PACAP analog with a C-terminal diaminodithiol (N_2S_2) chelator was synthesized (25–29) on a Wang resin using an ABI 341A peptide synthesizer (Applied Biosystems). Fmoc-Lys (ivDde) was first introduced at the C terminus of the peptide, followed by 4-aminobutyric acid (y-Aba). The 27-amino-acid PACAP sequence was then assembled by standard Fmoc coupling, with the final histidyl residue being a t-Boc–protected His(Trt) derivative. The capping t-Boc function was necessary to ensure that the N-terminal amino group remained protected during subsequent deprotection and coupling cycles performed at the y-amino group of the C-terminal lysine. The ivDde group at the C-terminal lysine was then selectively removed with 2% hydrazine, followed by successive additions of di-Fmoc-L-diaminopropionic acid and S-benzoylthioglycolic acid. The resulting protected diaminedithiol (NS-benzoyl)$_2$–containing PACAP peptide was cleaved from the resin using trifluoroacetic acid:water:phenol:thioanisole:ethanedithiol (82.5:5:5:5:2.5) and precipitated with diethyl ether.

The crude peptide was purified to homogeneity by reverse-phase high-pressure liquid chromatography (Waters) on a Vydac C4 column (5 μm, 10 × 250 mm). The mass of the analog-chelator construct was confirmed by electrospray mass spectrometry. Following the general synthetic scheme, TP3805 was prepared, purified, and characterized by American Peptide Co.

Kits were prepared aseptically in a laminar flow hood. All reagents were sterilized, including 10-mL glass vials, rubber caps, and aluminum sealing caps. All reagents were of analytic grade, were obtained from Fisher Scientific, Inc., and were used without further purification. The reagents added were 100 μg of SnCl$_2$·2H$_2$O (10 mg/mL, 0.05 M HCl) containing 100 μg of glucoheptonate (50 mg/mL, H$_2$O), 20 μg of TP3805 (10 mg/mL, and 0.1 M Na-acetate, pH 5), and 200 μL of 0.2 M glycine buffer, pH 9. The mixture was quickly frozen by placing the vials in an acetone and dry ice bath. The vials were then lyophilized for 4 h (SF50; Genevac), sterile N$_2$ gas was introduced in the chamber, and the vials were sealed, labeled, and stored at 4°C until use. The stability of the kits was checked by high-pressure liquid chromatography and for their ability to be labeled with ^{64}Cu.

Preparation of ^{64}Cu-TP3805

On the day of preparation, a kit vial was removed and brought to room temperature. The required quantity of ^{64}Cu solution (Washington University) was added to the vial (usually 222 MBq in < 20 μL of 0.1 M HCl), followed by 200 μL of sterile water. The vial was incubated at 50°C for 90 min. The solution was then diluted by the addition of 2 mL of sterile 0.9% NaCl.

The reaction mixture was analyzed by high-pressure liquid chromatography, with a reverse-phase Microbond column (Varian, Inc.) eluted with a linear 28-min gradient from 10% to 90% acetonitrile in aqueous 0.1% trifluoroacetic acid. (Labeling efficiency of ≥95% was considered the criterion for kit stability.) This procedure rendered a ^{64}Cu-TP3805 specific activity of 44.4 GBq (1.2 Ci/μmol).

Sterility Test

A required activity for patient injection was drawn into a sterile syringe and measured in a calibrated ionization chamber (CRC-15R; Capintec). Approximately 100 μL of the solution were added to 10 mL of tryptic soy broth and kept for 7 d in a humidified 5% CO$_2$ incubator at 37°C. The test tube was observed daily for 7 d to detect turbidity or microbial growth.

Patient Inclusion

Exploratory investigational new drug (eIND) number 101550 was assigned by the Food and Drug Administration. Approval was also obtained from the Institutional Review Board, Clinical Cancer Research Review Committee, and Radioactive Drug Research Committee. Nonpregnant women at least 18 y old and with newly diagnosed, histologically proven BC were enrolled. Image-guided percutaneous biopsy was performed 2–6 wk before this imaging procedure. All patients signed the Institutional Review Board–approved informed consent form. For this feasibility study, a Thomas Jefferson University biostatistician determined that 6 patients should be studied with PET and 13 with PEM. This determination was based on the assumption that ^{64}Cu-TP3805 will detect 80% of the lesions and that there will be 87% power to conclude that this agent is promising.

PET/CT Imaging

Each patient fasted for 6 h before ^{18}F-FDG injection. Before ^{18}F-FDG injection, blood glucose was monitored. All enrolled patients had glycemia levels well below 200 mg/dL. Each patient then received 370 MBq (10 mCi) of ^{18}F-FDG through an indwelling intravenous catheter and 1 h later underwent a PET/CT or PEM scan. PET/CT images were obtained with the patient supine and with a 2-min bed time using a Biograph-6 PET/CT scanner (Siemens, Inc.).

For ^{64}Cu-TP3805 imaging, patients neither fasted nor had their blood glycemic levels determined. ^{64}Cu-TP3805 was injected intravenously 2–30 d after the ^{18}F-FDG scan. As suggested by the Food and Drug Administration, 111 MBq (3 mCi) (±10%) were given to 2 patients, 127.5 MBq (3.5 mCi) (±10%) to 2 patients, and 148 MBq (4 mCi) (±10%) to the 2 remaining patients. For ^{64}Cu-TP3805 whole-body scans, the bed time was 4 min and images were obtained at 2 and 4 h after injection. A 4-min bed time for ^{64}Cu-TP3805 PET/CT imaging allowed compensating for the low β+ yield (19%) of ^{64}Cu. A 2- and 4-h whole-body imaging time was chosen to determine the optimal imaging time.

PEM Imaging

For PEM imaging (Solo I; Naviscan), each patient received 148 MBq (4 mCi) (±10%) of ^{64}Cu-TP3805 or 370 ± 29.6 MBq (10 ± 0.8 mCi) of ^{18}F-FDG through an indwelling intravenous catheter. Images were obtained for both breasts in mediolateral oblique and craniocaudal positions for 10 min per view. Data were collected at 15 min, 1 h, 2–3 h, and 5 h after injection to determine the optimal imaging time.

Vital signs for each PET/CT and PEM patient were monitored before injection and then for every 30 min until 4 h after injection. At the end of the injection, the syringe and the tubing were flushed with 5 mL of 0.9% NaCl and the radioactivity remaining was measured. During the course of the PEM study, patients were allowed to drink or eat if they wished.

Image Analysis

All images were read by 2 board-certified nuclear medicine physicians and a board-certified breast imaging physician. Image analysis was performed by a nuclear medicine fellow. For 6 patients with PET/CT images for both agents, standardized (maximal) uptake value (SUV) was calculated for the primary tumor site and metastatic lymph nodes and was compared for the respective radiotracers. Metabolic tumor volume was calculated using 50% isocontour geometry for comparison, as it is relatively a better parameter than SUV and may lead to a detection limit, if any, by the new agent.

For the 13 patients with PEM scans for both agents, PEM uptake values (PUVs) and tumor volumes were calculated for comparison. PEM (maximal) uptake value/background value (PUV/BGV) and mean SUV/PUV ratios were also calculated with each radiotracer and compared for evaluation.

RESULTS

^{64}Cu-TP3805 Radiochemical Purity and Sterility

For all ^{64}Cu-TP3805 preparations, the radiochemical purity as determined by high-pressure liquid chromatography averaged 97% ± 2%. The specific activity of the preparations averaged 44.4 GBq (1.2 Ci)/μmol. All preparations were sterile. The total radioactivity remaining in the syringe and the intravenous line was less than 5.5 MBq (150 μCi).

Patient Population

Patients were recruited in consecutive order as they consented. None of the patients had received any form of therapy for BC. The average age of the 6 PET/CT patients was 48.7 ± 6.2 y (range, 42–59 y). The average age of the 13 PEM patients was 54 ± 14.2 y (range, 26–80 y). Of the total of 19 patients, 2 patients experienced a flushing sensation that resolved within minutes without any medication. The demographic patient data are given in Table 1 together with critical results.

Image Analysis

In the whole-body PET/CT group, all 6 patients had histologically proven invasive ductal carcinoma. Five of these were estrogen receptor (ER)–positive, 1 ER-negative, 5 progesterone receptor (PR)–positive, 1 PR-negative, 2 human epidermal growth factor receptor 2 (HER$_2$)–positive, and 4 HER$_2$-negative. The quality for each image, irrespective of the quantity of ^{64}Cu-TP3805 the patients received, was excellent. Among these patients, there were a total of 10 lesions detected both by ^{18}F-FDG PET/CT and by ^{64}Cu-TP3805 PET/CT. Of these, 6 were primary (1 lesion in each patient) and 4 involved lymph nodes (2 in 1 patient [Fig. 1] and 1 each in the other 2 patients).

In the PEM group of 13 patients, 9 had histologically proven invasive ductal carcinoma, 2 had invasive lobular carcinoma, 1 had invasive papillary carcinoma, and 1 had high-grade mammary carcinoma. Of these, all 13 were ER-positive and none were ER-negative. Eight patients had PR-positive lesions and 5 had PR-negative. Of these, 2 were HER$_2$-positive and 7 were HER$_2$-negative, and for 4, the HER$_2$ status was indeterminate. One patient with invasive lobular carcinoma had 2 distinct lesions. These demographic data are given in Table 1.

The primary tumor volume in these 6 patents as determined by ^{18}F-FDG PET/CT scans ranged from 113 to 6,084 mm^3. The corresponding tumor volume as determined by the ^{64}Cu-TP3805 PET/CT scans ranged from 113 to 5,323 mm^3. The ^{64}Cu-TP3805 tumor volume was 90.6% ± 16.1% of the ^{18}F-FDG tumor volume. The volume range for the 4 lymph nodes was 28–509 mm^3 as determined by ^{18}F-FDG and 28–402 mm^3 as determined by ^{64}Cu-TP3805. The node volume as determined by ^{64}Cu-TP3805 was 86.2% ± 9.2% of that found by the ^{18}F-FDG scan.

All 6 primary lesions and 4 malignant lymph nodes were unequivocally detected by ^{64}Cu-TP3805 PET/CT imaging. ^{18}F-FDG PET/CT SUV range was 1.75–12.8 for the 6 primary lesions and 1.8–11.0 for the malignant lymph nodes. The corresponding ^{64}Cu-TP3805 PUV/BGV was 1.9–11.8 for the primary lesions and 2.4–4.9 for the lymph nodes. The ^{64}Cu-TP3805 PET/CT SUV was 92% ± 26.4% of the ^{18}F-FDG SUV for the primary lesions. The ^{64}Cu-TP3805 PET/CT SUV for the malignant lymph nodes was 89.8% ± 27% of the ^{18}F-FDG PET/CT SUV.

The whole-body images revealed liver uptake of ^{64}Cu-TP3805 (Fig. 1). The value was not quantified. The exact nature of this uptake is unknown. However, our preclinical data had indicated that liver uptake was 25.4% ± 1.74%, of which nearly 60% of the activity had the same molecular weight as TP3805, and that 7.5% of the activity was excreted in the feces within 24 h after injection (26). These preclinical data suggest that most of the liver uptake in patients may be due to intact ^{64}Cu-TP3805 and that a portion of this may be eliminated through feces.

For the 13 PEM patients, there were 14 primary lesions (2 in 1 patient), all of which were unequivocally delineated by ^{64}Cu-TP3805 (Fig. 2). The tumor volume as determined by ^{18}F-FDG PEM scans ranged from 141 to 3,818 mm^3. The tumor volume range, as calculated from the ^{64}Cu-TP3805 PEM scans, was 98 to 6,912 mm^3, 113% ± 37% of the ^{18}F-FDG values.

In PEM imaging, the ratios of PUV to BGV ranged from 2.6 to 11.6 for ^{18}F-FDG and from 2.7 to 11.8 for ^{64}Cu-TP3805. This is 97.7% ± 24.5% of the ^{18}F-FDG values.

Although the sample size is small, these data are important as they establish the utility of the ^{64}Cu-TP3805 probe for future clinical applications in patients with BC. Tumor uptake of ^{64}Cu-TP3805 as observed in PEM imaging was rapid. The average PUV/BGV ratio calculated for the 13 PEM patients from their 15-min PEM images was 3.1 ± 2.15 and remained steady at 3.2 ± 2.2 for images obtained 2–3 h after injection and at 3.3 ± 2.4 for images obtained 5 h after injection (Fig. 3). These values were not statistically significantly different ($P \geq 0.5$).

The tumor volume as determined by ^{18}F-FDG scans most likely represents the total volume of metabolically active malignant cells, and the tumor volume as determined by ^{64}Cu-TP3805 scans most likely represents the volume of cells that express VPAC1 receptors. The close congruity of tumor volumes (90.6% ± 16.1%

TABLE 1
Patient Demography and Analysis

Patient no.	Patient age (y)	MBq injected 18F-FDG	MBq injected 64Cu-TP3805	BC type	ER/PR/HER2	Maximal SUV/PUV/BGV 18F-FDG	Maximal SUV/PUV/BGV 64Cu-TP3805	Mean SUV/PUV/BGV 18F-FDG	Mean SUV/PUV/BGV 64Cu-TP3805	Tumor volume (mm³) 18F-FDG	Tumor volume (mm³) 64Cu-TP3805
PET/CT											
1	42	370	110.6	IDC	+/+/−	12.8 LN-1.11.0	6.8 LN-1.4.9	6.5 LN-1.5.5	3.48 LN-1.2.4	6,084 LN-1.28	5,323 LN-1.28
2	46	370	107.3	IDC	+/+/−	5.5 LN-1.1.8 LN-2.2.3	7.0 LN-1.2.6 LN-2.2.4	3.1 LN-1.3.1 LN-2.0.89	3.8 LN-1.3.4 LN-2.1.2	5,028 LN-1.59 LN-2.38	4,714 LN-1.49 LN-2.31
3	49	370	125.8	IDC	+/+/−	2.2	2.1	1.2	0.9	113	113
4	52	370	125.8	IDC	−/−/+	5.2	4.7	2.8	2.3	2,614	1,726
5	44	370	144.3	IDC	+/+/+	1.75 LN-1.5.2	1.9 LN-1.4	0.9 LN-1.1.3	0.9 LN-1.2.1	1,385 LN-1.509	1,018 LN-1.402
6	59	370	140.6	IDC	+/+/−	5.0	4.4	2.6	2.7	2,617	2,651
PEM											
1	68	370	144.6	IDC	+/+/?	6.7	6.2	5.2	5.6	509	402
2	57	370	140.6	IDC	+/−/+	9.6	7.9	8.5	6.9	3,818	4,714
3	80	370	144.6	IDC	+/+/−	1.9	3.0	2.3	2.4	141	98
4	46	370	142.5	ILoC	+/+/−	4.3	3.7	4.9	3.4	509	346
5	39	370	159.1	IDC	+/−/?	5.1	4.7	5.7	4.9	785	1,357
6	59	370	162.8	IDC	+/+/?	11.6	11.8	13.6	11.9	7,812	6,912
7	39	370	144.3	IDC	+/+/−	2.9	2.2	3.4	1.8	3,178	2,828
8	55	370	151.7	ILoC	+/+/−	3.0	3.3	2.6	2.7	445	549
						3.1	3.5	2.5	2.7	395	497
9	52	370	159.1	IPaC	+/−/+	7.3	5.8	6.7	6.3	1,847	1,357
10	58	370	140.6	IDC	+/+/−	6.2	5.4	5.7	4.8	1,436	1,767
11	55	370	144.3	IDC	+/−/?	2.6	3.1	2.9	3.3	268	381
12	68	370	155.4	IDC	+/+/−	2.7	3.1	2.9	2.9	1,150	1,767
13	26	370	151.7	HGMC	+/−/−	4.5	2.7	3.8	2.9	696	1,150

IDC = invasive ductal carcinoma; LN = lymph node; ILoC = invasive lobular carcinoma; IPaC = invasive papillary carcinoma; HGMC = high-grade mammary carcinoma.
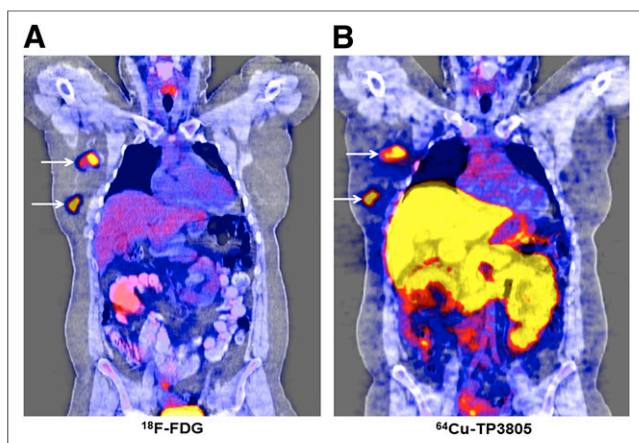
FIGURE 1. A 42-y-old woman with histologically proven invasive ductal carcinoma (ER-positive, PR-positive, HER$_2$-negative) had positive ^{18}F-FDG PET/CT findings (A) that delineated primary mass in right breast and pair of lymph nodes in axilla. Same lesions were also clearly visible on whole-body ^{64}Cu-TP3805 PET/CT scan (B) obtained 2 h after administration of 140.6 MBq (3.8 mCi) of ^{64}Cu-TP3805 (^{18}F-FDG equivalent, 28,860 kBq [780 μCi]).

and 113% ± 37%, respectively) by the 2 agents indicates that a significantly large number of metabolically active malignant cells express VPAC1 receptors and vice versa.

By design, the ^{64}Cu-TP3805 received by all 19 patients ranged from 107.3 to 162.8 MBq. Given that the positron emission of ^{64}Cu is only 19%, compared with 97% for ^{18}F-FDG, the effective ^{64}Cu-TP3805 dose ranged from 21 to 33 MBq, less than one tenth the dose of ^{18}F-FDG. Despite this small amount of tracer, the ^{64}Cu-TP3805 image quality was excellent, both for PET/CT images (Fig. 1) and for PEM images (Figs. 2 and 3). All malignant lesions ($n = 20$), including the malignant lymph nodes ($n = 4$), were clearly delineated by ^{64}Cu-TP3805.

Chemical Toxicity and Radiation Exposure

^{64}Cu is a rapidly emerging β+ radionuclide. It is used in humans for PET imaging (American College of Radiology Imaging Network [ACRIN] 6682, phase II trial, 2012) (28–30). ^{64}Cu has a t$_{1/2}$ (12.8 h) long enough to be dispatched throughout the country but not so long as to deliver an excessive radiation dose to patients after imaging. ^{64}Cu is produced in large quantities on small cyclotrons, and its chemistry is well known. In our PEM studies, 13 patients received 143.19 MBq (3.87 mCi) (±0.2%) and an estimated dose of 2.52 mSv to the whole body and 36.5 mSv to the liver (target organ, eIND 101550). Table 2 shows data for ^{64}Cu-TP3805 and for other BC imaging agents, such as those used in the ACRIN study and an agent that has been used in humans since 1970, ^{67}Ga. Data demonstrate that radiation exposure induced by ^{64}Cu-TP3805 is less than that induced by the well-established radiotracers and the ACRIN-promoted ^{64}Cu-ATSM (Table 2) (30–34).

Lewis et al. (34) demonstrated that the metal ions in a dose of ^{64}Cu more than 6 times greater than that we propose (same manufacturer) are not toxic. In addition, our data on rabbits receiving a 1,000× dose (adjusted to body weight) of decayed ^{64}Cu-TP3805 did not elevate c-AMP, alter blood chemistry, or change liver enzymes. No toxicity was observed in any of the 19 patients who received ^{64}Cu-TP3805 (eIND 101550).

DISCUSSION

During the past few decades, advances in imaging BC have contributed extensively to its early detection. Early detection with mammographic screening has been proven to decrease BC mortality. However, mammography and all other breast imaging modalities produce many suggestive findings, only about 20% of which will actually be malignant but all of which will require biopsy for diagnosis. In the United States each year, an estimated 1.6 million biopsies are performed. More than 1.3 million of these result in benign pathology, yet they produce patient morbidity and cost billions of dollars to the health care system (2).

A compelling need therefore exists for a biomolecule that will not only detect BC early but also distinguish these malignancies from benign lesions accurately and noninvasively. Such a biomolecule could minimize the need for invasive biopsies and could significantly reduce health care costs.

We hypothesized that VPAC1 oncogene product, which is overexpressed on all BC cells at the onset of oncogenesis irrespective of their hormonal status, will serve as an excellent biomarker for early and accurate detection of BC. Furthermore, since VPAC1 receptors are not overexpressed on cells of normal breast tissue or benign masses, the probe targeting VPAC1 receptors will image only malignant lesions, not benign masses. We chose to use ^{64}Cu as the probe because of the relatively inferior quality of ^{99m}Tc-TP3654 (20); the poor resolution of γ-cameras, which may prevent us from imaging lesions less than 6 mm in diameter; and the uncertainty about the supply of ^{99m}Tc. Furthermore, for ^{64}Cu, the resolution of the PEM Solo II (Naviscan) is 2.4 mm and that of the Clear-PEM (Clear Crystal Collaboration at CERN, Geneva, Switzerland) is 1.3 mm. The resolution of the modern BC imaging camera Dilon 6800 (Dilon Technologies) is 6 mm, and that of the Discovery NM 750b (GE Healthcare) is 3.5 mm (20,35).

Our PEM image quality is much better with ^{64}Cu-TP3805 than with ^{99m}Tc-TP3654 (20). Thus, the ^{64}Cu availability, elimination of CT radiation in PET/CT, high PEM resolution, and better image quality make a compelling case for using ^{64}Cu-TP3805 for PEM. Our preliminary data on MMTVneu mice that spontaneously grew
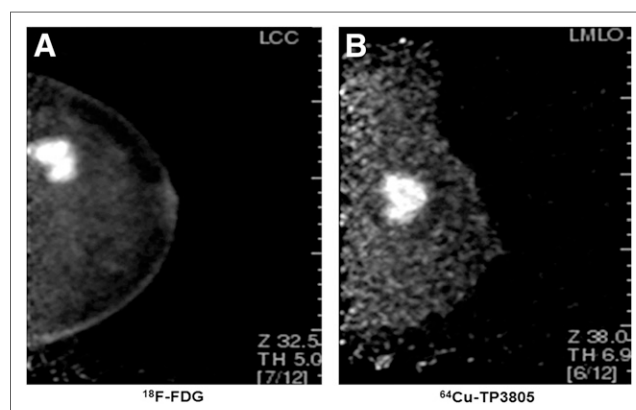

FIGURE 2. ^{18}F-FDG PEM scan (A, 370 MBq [10 mCi]) of left breast of 39-y-old woman was obtained 1 h after injection, and ^{64}Cu-TP3805 PEM scan (B, 159.1 MBq [4.3 mCi]; ^{18}F-FDG equivalent, 31,820 kBq [860 μCi]) was acquired 15 min after injection. PUV/BGV ratios for lesion (invasive ductal carcinoma, ER-positive, PR-positive, HER$_2$-negative) were 2.9 for ^{18}F-FDG and 2.2 (lowest of series) for ^{64}Cu-TP3805.
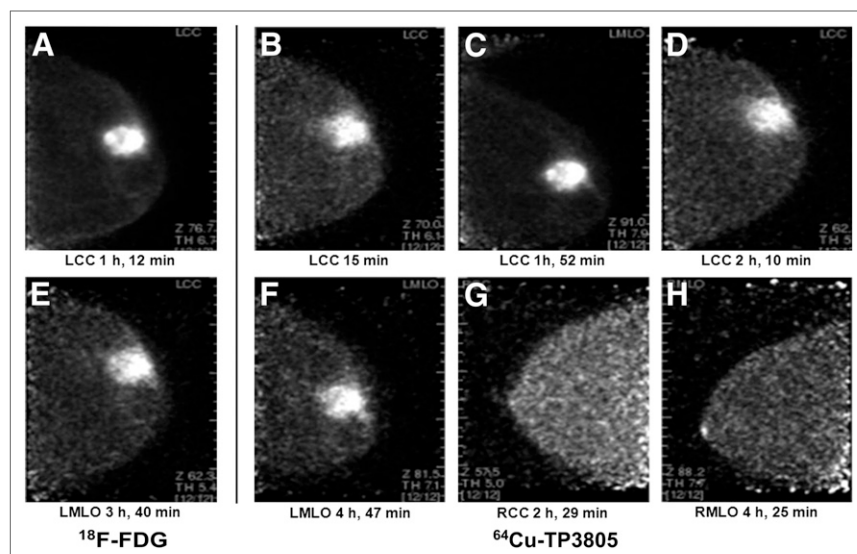
FIGURE 3. One-hour ^{18}F-FDG PEM scan (A, 370 MBq [10 mCi]) and longitudinal ^{64}Cu-TP3805 PEM scans (B–F, 162.8 MBq, (4.4 mCi]); ^{18}F-FDG equivalent, 32,560 kBq [880 μCi]) of 59-y-old woman 15 min, 1 h 52 min, 2 h 10 min, 3 h 40 min, and 4 h 47 min after injection. She had invasive ductal carcinoma of left breast (ER-positive, PR-positive, HER$_2$-indeterminate). ^{64}Cu-TP3805 PEM images of normal right breast (G and H) 2 h 20 min and 4 h 25 min after injection are also given. ^{18}F-FDG PUV was 11.6. ^{64}Cu-TP3805 PUV/BGV ratio was 11.9 and remained nearly unchanged for all images (C–F) obtained at various time points after injection. LCC = left craniocaudal; LMLO = left mediolateral oblique; RCC = right craniocaudal; RMLO = right mediolateral oblique.

BC and mimicked the pathophysiology of human BC validated our hypothesis in which we had used ^{64}Cu-TP3805 as the specific probe for PET imaging of primary as well as metastatic BC (26). Furthermore, in this study, ^{64}Cu-TP3805 did not accumulate in lesions that were shown by histology to be nonmalignant and did not express VPAC1 receptors by reverse transcription polymerase chain reaction (26).

In this present human investigation, designed not as an efficacy study but merely as a feasibility and safety study, ^{64}Cu-TP3805 imaged all 20 primary malignant tumors in 19 patients (1 patient had 2 lesions and the remaining 18 had 1 each). In addition, in whole-body PET/CT imaging, 4 involved sentinel lymph nodes (2 in 1 patient and 1 each in the other 2 patients) were also delineated clearly. Although all lesions were also delineated by ^{18}F-FDG, in large studies ^{18}F-FDG is known to be nonspecific, to miss up to 30% of BC lesions, and to not be able to distinguish benign lesions from malignant masses.

In this small patient study, 2 other observations were made that are noteworthy. The first is that the ^{64}Cu-TP3805 uptake was

rapid, 15 min after injection. This suggests in principle that, instead of using ^{64}Cu with a $t_{1/2}$ of 12.8 h, we can use generator-produced ^{68}Ga with a $t_{1/2}$ of 68 min. The positron emission of ^{68}Ga is 88%, more than 4 times greater than that of ^{64}Cu. This will permit us to administer less than 150 MBq (~4 mCi) of ^{68}Ga without compromising image quality yet significantly reducing radiation burden to the subjects. Images can be obtained 15 min after injection without requiring patient fasting or monitoring of their blood glycemic level.

Second, we observed that the PUV/BGV ratios of images obtained in the 15 min after injection did not significantly alter during up to 5 h of imaging, suggesting that ^{67}Cu-TP3805 might be used as a therapeutic agent without alteration in the chemistry of its preparation. ^{67}Cu (β−, 100%; $t_{1/2}$, 2.44 d) is considered a radionuclide of therapeutic importance (36). Although it is not yet available commercially, many facilities in the nation are capable of producing it.

From this small feasibility study, it is also reasonable to point out 2 minor but important observations. One is the tumor volume congruity (^{18}F-FDG vs. ^{64}Cu-TP3805), which indicates that most metabolically active malignant cells express VPAC1 receptors and vice versa. The other observation suggests that irrespective of their hormonal status (Table 1) all tumors were unequivocally delineated by ^{64}Cu-TP3805. These observations need to be substantiated in larger clinical studies.

Because the patient population was small, it is premature to comment on the sensitivity and specificity of ^{64}Cu-TP3805. Nevertheless, ^{64}Cu-TP3805 detected all primary lesions (100%), delineated all involved sentinel lymph nodes (100%), and is worthy of further investigation in patients for whom biopsy of suggestive breast lesions is recommended, to evaluate its ability to distinguish benign masses from malignant lesions by PET or PEM imaging (37).

CONCLUSION

There is a compelling need for a biomolecule that will distinguish malignant from benign lesions noninvasively. ^{64}Cu-TP3805 promises to be such an agent. In this feasibility study,

TABLE 2
Comparative Radiation Dosimetry

Procedure	Effective dose (mSv)	Liver dose (mSv)	Reference
^{64}Cu-TP3805 (148 MBq [4 mCi])	2.5	36.5	Gingold E, eIND 101550
^{18}F-FDG PET/CT (^{18}F, 370 MBq [10 mCi])	31.9	5.8	*31*
^{99m}Tc-sestamibi (1,110 MBq [30 mCi])	9.4	6.0	*32*
^{18}F-FDG PET/PEM without CT (^{18}F, 370 MBq [10 mCi])	7.8	5.8	*32*
^{67}Ga-citrate (370 MBq [10 mCi])	39	69	*33*
^{64}Cu-ATSM (925 MBq [25 mCi])	33.3	361	*34*

^{64}Cu-TP3805, which targets VPAC1 oncogene receptors, unequivocally detected all malignant breast lesions by PET/CT and PEM and delineated all involved lymph nodes. These results warrant further studies in patients to validate the hypothesis that ^{64}Cu-TP3805 will help reduce the number of unnecessary biopsies, minimize patient anxiety, and reduce health care cost.

REFERENCES

1. DeSantis C, Siegel R, Bandi P, et al. Breast cancer statistics, 2011. *CA Cancer J Clin.* 2011;61:409–418.
2. Elter M, Schulz-Wendtland R, Wittenberg T. The prediction of breast cancer biopsy outcomes using two CAD approaches that both emphasize an intelligible decision process. *Med Phys.* 2007;34:4164–4172.
3. Uematsu T, Sano M, Homma K. False-positive helical CT findings of multifocal and multicentric breast cancer: is attenuation of tumor useful for diagnosing enhanced lesions? *Breast Cancer.* 2002;9:62–68.
4. Berg WA, Gutierrez L, NessAiver MS, et al. Diagnostic accuracy of mammography, clinical examination, US, and MR imaging in preoperative assessment of breast cancer. *Radiology.* 2004;233:830–849.
5. Ruibal A, Maldinado A, Sanchez Salmon A, et al. ^{18}FDG-PET in patients with situ breast carcinomas: a cause of false negative results. *Med Clin (Barc).* 2008;130:332–333.
6. Tse GM, Yang W. Sonographic, mammographic, and histopathologic correlation of symptomatic ductal carcinoma in situ. *AJR.* 2004;182:101–110.
7. Elmore JG, Armstrong K, Lehman CD, et al. Screening for breast cancer. *JAMA.* 2005;293:1245–1256.
8. Ghai S, Muradali D, Bukhanov K, et al. Nonenhancing breast malignancies on MRI: sonographic and pathologic correlation. *AJR.* 2005;185:481–487.
9. Chagpar AB, Middleton LP, Sahin AA, et al. Accuracy of physical examination, ultrasonography, and mammography in predicting residual pathologic tumor size in patients treated with neoadjuvant chemotherapy. *Ann Surg.* 2006;243:257–264.
10. Xu HB, Li L, Xu Q. Tc-99m sestamibi scintimammography for the diagnosis of breast cancer: meta-analysis and meta-regression. *Nucl Med Commun.* 2011;32:980–988.
11. Xue DQ, Qian C, Yang L, Wang XF. Risk factors for surgical site infections after breast surgery: a systematic review and meta-analysis. *Eur J Surg Oncol.* 2012;38:375–381.
12. Printz C. Unnecessary breast cancer biopsies still performed. *Cancer.* 2010;116:1619.
13. Reubi JC, Laderach U, Waser B, et al. Vasoactive intestinal peptide/pituitary adenylate cyclase-activating peptide receptor subtypes in human tumors and their tissues of origin. *Cancer Res.* 2000;60:3105–3112.
14. Zia H, Hida T, Jakowlew S, et al. Breast cancer growth is inhibited by vasoactive intestinal peptide, (VIP) hybrid, a synthetic VIP receptor antagonist. *Cancer Res.* 1996;56:3486–3489.
15. Leyton J, Gozes Y, Pisegna J, et al. PACAP(6-38) is a PACAP receptor antagonist for breast cancer cells. *Breast Cancer Res Treat.* 1999;56:177–186.
16. Moody TW, Gozes I. Vasoactive intestinal peptide receptors: a molecular target in breast and lung cancer. *Curr Pharm Des.* 2007;13:1099–1104.
17. Valdehita A, Bajo AM, Fernández-Martínez AB, et al. Nuclear localization of vasoactive intestinal peptide (VIP) receptors in human breast cancer. *Peptides.* 2010;31:2035–2045.
18. Valdehita A, Carmena MJ, Bajo AM, Prieto JC. RNA interference-directed silencing of VPAC1 receptor inhibits VIP effects on both EGFR and HER2 transactivation and VEGF secretion in human breast cancer cells. *Mol Cell Endocrinol.* 2012;348:241–246.
19. Chakder S, Rattan S. The entire vasoactive intestinal polypeptide molecule is required for the activation of the vasoactive intestinal polypeptide receptor: functional and binding studies. *J Pharmacol Exp Ther.* 1993;266:392–399.
20. Thakur ML, Marcus CS, Saeed S, et al. 99m Tc-labeled vasoactive intestinal peptide analog for rapid localization of tumors in humans. *J Nucl Med.* 2000;41:107–110.
21. Pallela VR, Thakur ML, Chakder S, et al. ^{99m}Tc-labeled vasoactive intestinal peptide receptor agonist: functional studies. *J Nucl Med.* 1999;40:352–360.
22. Kolan HR, Pallela V, Thakur ML. Tc-99m labeled vasoactive intestinal peptide, (VIP): preparation and preliminary evaluation. *J Labelled Comp Radiopharm.* 1997;40:455–457.
23. Thakur ML, Aruva M, Gariepy J, et al. Imaging oncogene overexpression using ^{64}Cu-VIP analog: comparison with ^{99m}Tc-VIP analog. *J Nucl Med.* 2004;45:1381–1389.
24. Zhang K, Aruva M, Shanthly N, et al. Vasoactive intestinal peptide (VIP) and pituitary adenylate cyclase activating peptide (PACAP) receptor specific peptide analogues for PET imaging of breast cancer: in vitro/in vivo evaluation. *Regul Pept.* 2007;144:91–100.
25. Thakur ML. Genomic biomarkers for molecular imaging: predicting the future. *Semin Nucl Med.* 2009;39:236–246.
26. Thakur ML, Devadhas D, Zhang K, et al. Imaging spontaneous MMTVneu transgenic murine mammary tumors: targeting metabolic activity versus genetic products. *J Nucl Med.* 2010;51:106–111.
27. Zhang K, Aruva MR, Shanthly N, et al. PET imaging of VPAC1 expression in experimental and spontaneous prostate cancer. *J Nucl Med.* 2008;49:112–121.
28. Anderson CJ, Dehdashti F, Cutler PD, et al. ^{64}Cu-TETA-octreotide as a PET imaging agent for patients with neuroendocrine tumors. *J Nucl Med.* 2001;42:213–221.
29. Lewis J, Laforest R, Buettner T, et al. Copper-64-diacetyl-bis(N4-methylthiosemicarbazone): an agent for radiotherapy. *Proc Natl Acad Sci USA.* 2001;98:1206–1211.
30. Pfeifer A, Knigge U, Mortensen J, et al. Clinical PET of neuroendocrine tumors using ^{64}Cu-DOTATATE: first-in-humans study. *J Nucl Med.* 2012;53:1207–1215.
31. Huang B, Law MW, Khong PL. Whole-body PET/CT scanning: estimation of radiation dose and cancer risk. *Radiology.* 2009;251:166–174.
32. Hendrick RE. Radiation doses and cancer risks from breast imaging studies. *Radiology.* 2010;257:246–253.
33. MIRD-dose estimate report no. 2: summary of current radiation dose estimates to humans from ^{66}Ga-, ^{67}Ga-, ^{68}Ga-, and ^{72}Ga-citrate. *J Nucl Med.* 1973;14:755–756.
34. Lewis JS, Laforest R, Dehdashti F, et al. An imaging comparison of ^{64}Cu-ATSM and ^{60}Cu-ATSM in cancer of the uterine cervix. *J Nucl Med.* 2008;49:1177–1182.
35. Moadel RM. Breast cancer imaging devices. *Semin Nucl Med.* 2011;41:229–241.
36. Knogler K, Grünberg J, Zimmermann K, et al. Copper-67 radioimmunotherapy and growth inhibition by anti-L1-cell adhesion molecule monoclonal antibodies in a therapy model of ovarian cancer metastasis. *Clin Cancer Res.* 2007;13:603–611.
37. Berg WA, Weinberg IN, Narayanan D, et al. High-resolution fluorodeoxyglucose positron emission tomography with compression ("positron emission mammography") is highly accurate in depicting primary breast cancer. *Breast J.* 2006;12:309–323.